Accepted Manuscript

Title: Can contaminated waters or wastewater be alternative sources for technology-critical elements? The case of removal and recovery of lanthanides

Authors: Elisabete Luís Afonso, Lina Carvalho, Sara Fateixa, Carlos Oliveira Amorim, Vitor S. Amaral, Carlos Vale, Eduarda Pereira, Carlos Manuel Silva, Tito Trindade, Cláudia Batista Lopes

PII: S0304-3894(19)30798-8
DOI: https://doi.org/10.1016/j.jhazmat.2019.120845
Article Number: 120845

Reference: HAZMAT 120845

To appear in: *Journal of Hazardous Materials*

Received date: 18 March 2019
Revised date: 25 June 2019
Accepted date: 28 June 2019

Please cite this article as: Afonso EL, Carvalho L, Fateixa S, Amorim CO, Amaral VS, Vale C, Pereira E, Silva CM, Trindade T, Lopes CB, Can contaminated waters or wastewater be alternative sources for technology-critical elements? The case of removal and recovery of lanthanides, *Journal of Hazardous Materials* (2019), https://doi.org/10.1016/j.jhazmat.2019.120845

Can contaminated waters or wastewater be alternative sources for technology-critical elements? The case of removal and recovery of lanthanides

Elisabete Luís Afonso[a], Lina Carvalho[b], Sara Fateixa[a], Carlos Oliveira Amorim[c], Vitor S. Amaral[c], Carlos Vale[d], Eduarda Pereira[e], Carlos Manuel Silva[a], Tito Trindade[a] and Cláudia Batista Lopes*[a]

[a] *CICECO - Aveiro Institute of Materials, Department of Chemistry, University of Aveiro, 3810-193 Aveiro, Portugal*

[b] *Central Laboratory of Analysis (LCA), University of Aveiro, Campus de Santiago, 3810-193 Aveiro, Portugal*

[c] *CICECO – Aveiro Institute of Materials, Department of Physics, University of Aveiro, 3810-193 Aveiro, Portugal*

[d] *CIIMAR - Interdisciplinary Centre of Marine and Environmental Research, Av. General Norton de Matos s/n 4450-208 Matosinhos, Portugal*

[e] *QOPNA & LAQV-REQUIMTE, Department of Chemistry, University of Aveiro, 3810-193 Aveiro, Portugal.*

* Corresponding authors (claudia.b.lopes@ua.pt)

Graphical abstract

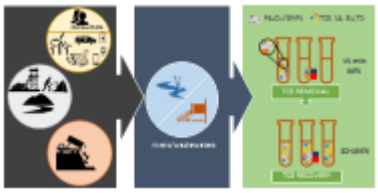

Highlights

- Fabrication of a dual function magnetic hybrid nanocomposite.
- Possibility of remove and recover lanthanoids from water.
- High removal efficiency of the composite in alkaline media.
- In competitive media, the composite showed preferential removal for Eu and Tb.
- The consecutive application of the composite highlights its efficient recyclability.

Abstract

Technology critical elements (TCE) are considered the vitamins of nowadays technology. Factors such as high demand, limited sources and geopolitical pressures, mining exploitation and its negative impact, point these elements as new emerging contaminants and highlight the importance for removal and recycling TCE from contaminated waters. This paper reports the synthesis, characterization and application of hybrid nanostructures to remove and recover lanthanides from water, promoting the recycling of these high value elements. The nanocomposite combines the interesting properties of graphite nanoplatelets, with the magnetic properties of magnetite, and exhibits good sorption properties towards La(III), Eu(III) and Tb(III). The sorption process was very sensitive to solution pH, evidencing that electrostatic interactions are the main binding mechanism involved. Removal efficiencies up to 80% were achieved at pH 8, using only 50 mg/L of nanocomposite. In ternary solution, occurred a preferential removal of Eu(III) and Tb(III). The equilibrium evidenced a rare but interesting behaviour, and as a proof-of-concept the

recoveries and reutilization rates, at consecutive cycles, highlight the recyclability of the composite without loss of efficiency. This study evidences that surface charge and the number of active sites of the composite controls the removal process, providing new insights on the interactions between lanthanoids and magnetic-graphite-nanoplatelets.

Keywords

Lanthanum; Europium; Terbium; Adsorption; Graphite Nanoplatelets; Magnetite nanoparticles.

1. Introduction

There has been great concern about future supplies and increasingly cost of trace elements that are essential for key technologies such as renewable energy, electronics, energy efficiency and aerospace industry[1,2]. These elements are often called technology-critical elements (TCE) due to their increasing use and demand for high-technology advances, and at the same time due to their vulnerability to politically or economically driven fluctuations in supply[1,3,4]. According to Filella[3], the group of TCE include most of the rare-earth elements (REE), the platinum group elements, tantalum (Ta), niobium (Nb), gallium (Ga), germanium (Ge), indium (In), thallium (Tl) and tellurium (Te). In particular, lanthanoids have been recognised for a long time as crucial elements in diverse technologies due to important properties conferred to materials and devices, such as luminescent and magnetic behaviour[4].

The high demand and poor resource base of lanthanoids enforce the development of new ways to recover these elements from wastewaters and aquatic systems[3]. The presence of lanthanoids in rivers, wastewaters and effluents is typically in ultra-trace concentrations[5]. However, this scenario is changing rapidly and substantially. The current use of these elements in

new technological products is resulting in significant changes in the processes associated with their natural environmental cycle at the Earth's surface due to increased mining activities and use in a variety of products[1,6]. Currently, at all stages of their life cycle, these elements and their compounds can be released into the environment. Some works reported the presence of lanthanoids in rivers and wastewaters[6,7], and solid wastes[8–10]. These solid wastes and streams could become economically attractive secondary sources of TCE[11], and thus, there is an opportunity to explore the efficient recovery of these elements from waters and wastewaters, mitigating also the hazardous consequences of the mining process.

Graphite-like nanoplatelets (GNPs) have attracted great attention in the past decade, as a viable and inexpensive material for many engineering applications, given the excellent in-plane mechanical, structural, thermal, and electrical properties of graphite[12], and have been recently used in composite materials[13–15], sensors[16,17], membranes[18,19], adsorption of dyes and CO_2[20,21], batteries[22], among others[23,24]. Our own interest in the preparation of magnetic nanomaterials as new adsorbents[25–31] for water treatment applications led us to explore here the preparation of magnetic composites based on graphite nanoplatelets. Hence, the hybrid structures described here combine the sorption properties of GNPs with the magnetic properties of magnetite (Fe_3O_4), thereby conferring ability for magnetic separation of the sorbents when exposed to an external magnetic gradient. Moreover, in line with the high demand of TCE for high-tech applications, these nanocomposites are also interesting as alternative and less expensive carbon-based adsorbents for lanthanoids. In this study, we investigate the application of magnetite-GNPs composites to capture selected TCE (La, Eu and Tb), from unary and ternary solutions, towards the development of a simple and environmentally friendly procedure, with potential for future application in the recovery of TCE from industrial or other water systems.

2. Experimental

2.1. Chemicals

The reagents used were analytical reagent grade and were used without further purification. For the synthesis of the composite, graphite flakes (EDM 99.95%), dimethylformamide (DMF), potassium hydroxide (KOH), potassium nitrate (KNO_3), iron sulphate ($FeSO_4 \cdot 7H_2O$), nitric acid (HNO_3, 63%), hydrochloride acid (HCl, 30%) and ethanol (C_2H_5OH, PA) were purchase from commercial sources. For the removal and recovery essays of TCE, ultra-pure water (UPW) was used for the solutions preparation. Certified commercial standards solutions of lanthanum (La_2O_3 in HNO_3 4%), europium (Eu_2O_3 in HNO_3 4%) and terbium (Tb_3O_7 in HNO_3 5%) with concentration 1002±1 mg/L, were purchased from SCP Science. In such acidic conditions, the lanthanide oxides dissolve into the respective cations and the counter anions present are nitrate species.

2.2. Materials synthesis

2.2.1.Graphite nanoplatelets and Fe_3O_4 nanoparticles

The GNPs were obtained by ultrasonic treatment (Sonics Vibra Cell Sonicator, VC70, 130 W, 20 kHz) of graphite in DMF. The Fe_3O_4 NPs were prepared by oxidative hydrolysis of $FeSO_4$ in alkaline media[32]. Details can be found in Supplementary Material (SM).

2.2.2.Fe_3O_4/GNPs composite

The Fe_3O_4/GNPs was prepared by using a modification of the electrostatic assembly methodology proposed by Han and co-authors[33]. GNPs (100 mg) were dispersed in UPW under sonication (Sonics Vibra Cell Sonicator VC70, 130 W, 20 kHz) for 1h. In parallel to this, 100 mg of Fe_3O_4 NPs were suspended in 0.1 mol/L HNO_3 solution (100 mL) and then added to the GNPs

dispersion, under sonication during 1h. The final composite, denoted by Fe_3O_4/GNPs was collected using a NdFeB magnet, washed with UPW and ethanol and dried at 40°C in an oven.

2.3. Materials characterization

The powder XRD data were collected using a Phillips X'Pert MPD diffractometer using Cu-Kα radiation. Transmission electron microscopy (TEM) images were recorded by a 200 kV Hitachi H9100 Instrument. The FTIR spectra of the samples in KBr pellets, before and after the TCE sorption were recorded using a Mattson 7000 FTIR spectrometer. Raman spectra were obtained using a Raman confocal microscope (alpha 300 RAS+, WITec, Germany), equipped with a Nd:YAG laser operating at 532nm. Magnetic measurements were performed using a Quantum Design MPMS3 SQUID-VSM. The zeta potential experiments were conducted with a Malvern Zetasizer Nano ZS particle analyser (Malvern Instruments Ltd).

2.4. Removal and Recovery of Technology-Critical Elements

2.4.1.Removal of Technology-Critical Elements from water

All sorption essays were carried out in unary or/and ternary solutions of La(III), Eu(III) and Tb(III) with an initial element concentration of 100 µg/L, a value chosen based on reported concentrations for lanthanides in rivers and waste waters (Table 1, SM). The unary and ternary solutions were prepared by adding the required volume of certified reference standard solutions to UPW. Batch experiments were conducted at a maximum period of 24h in Schott© glass flasks at 22°C, with mechanical stirring (250 rpm). The capability of the composite to remove TCE from water was evaluated for different pH values (2 to 10), by exposing 5 mg of Fe_3O_4/GNPs to 100 mL of ternary solutions of La(III), Eu(III) and Tb(III). At 0 and 24h, 10 mL of water were collected and

acidified to pH<2 with HNO_3 (65%) for preservation and stored at 4°C until quantification. Results were expressed in terms of removal efficiency (R_A, eq. 1):

$$R_A = (C_{A0} - C_A/C_{A0}) \times 100 \quad (1)$$

where C_{A0} and C_A (both µg/L) are the initial and at time *t* concentration of each element (A) in solution.

Kinetics of TCE removal process was studied by exposing 10 and 50 mg of Fe_3O_4/GNPs to 1 L of unary and ternary solutions of La(III), Eu(III) and Tb(III) (pH adjusted to 7.5±0.2), and by collecting 10 mL of water at pre-defined times (0, 5, 10, 15, 20, 25, 30 and 45 min, and 1, 1.5, 2, 4, 6 and 24h). After collection, water samples were preserved and stored as previously described. The kinetic results were expressed in terms of normalized concentration (C_A/C_{A0}) and solid loadings (q_A, eq. 2):

$$q_A = (C_{A0} - C_A) \times (V/m) \quad (2)$$

where V and m are respectively, the volume of solution (L) and the mass of composite (mg). The kinetics of La(III), Eu(III) and Tb(III) removal from unary and ternary solutions was investigated and the experimental results were interpreted by three of the most used kinetic models[34–37]: pseudo-first order equation[38], pseudo-second order equation[39] and Elovich model[40].

Equilibrium of TCE removal process was studied by exposing different amounts (2, 4, 8, 12, 16, 20, 30, 40 and 60 mg/L) of composite to unary and ternary solutions of La(III), Eu(III) and Tb(III) (pH adjusted to 7.5±0.2) during 24h. At 0 and 24h, 10 mL of water were collected, preserved and stored as mentioned previously. Results were expressed as solid loading at equilibrium, using Eq. 2 where $q_A = q_{A,e}$ and $C_A = C_{A,e}$. The Freundlich model[41] was used to fit the equilibrium data. Detailed data analyses and model information for kinetics and isotherms are described in SM.

All experiments were performed in duplicate and with controls (UPW spiked with TCE in the absence of composite) running in parallel with the experiments and under the same experimental

conditions. Quantification of TCE in water samples was performed by inductively coupled plasma optical emission spectroscopy (ICP-OES, Horiba Jobin Yvon Activa M). Calibration curves were obtained using standards within the concentration range of 10–100 µg/L prepared by diluting a certified standard solution in 2% HNO_3. The limit of quantification of the method for all elements was 10 µg/L. All glassware used in the removal studies was prewashed (HNO_3 25%, Merck, 24h), and then rinsed plentifully with UPW.

2.4.2.Recovery of Technology-Critical Elements from Fe_3O_4/GNPs

After 24h exposition of 25 mg of composite to 100 mL of ternary solutions of La(III), Eu(III) and Tb(III), with an initial element concentration of 100 µg/L, the recovery of the elements was studied by contacting the composite to 0.1 mol/L HNO_3 solution (eluent solution), for 24h. The quantification of La(III), Eu(III) and Tb(III) in the TCE solution before and after exposition to the Fe_3O_4/GNPs and in the eluents solution, after magnetic separation of the composite was carried out as described previously. Afterward, the sorbent was neutralized by UPW and reconditioned for consecutive sorption/desorption cycles.

3. Results and discussion

3.1. Fe_3O_4/GNPs characterization

A three-step procedure was employed here for the fabrication of Fe_3O_4/GNPs. The isoelectric point of the composite was found at pH 5.2 (Figure 1, SM). TEM images of the final composite confirm the presence of nearly spherical Fe_3O_4 NPs, average size below 100 nm, attached onto GNPs, the lighter shaded substrate (Figure 1). For sake of comparison, TEM images for GNPs and Fe_3O_4 samples are also shown. The powder XRD of the composite revealed the presence of crystalline magnetite and GNPs (Figure 2, SM). The intense peak at $2\theta=26.56°$ corresponds to the

interlayer (002) planes distanced 0.34 nm in the graphitic structure, and the remaining XRD peaks observed are assigned to the inverse spinel structure of magnetite as indicated by the respective Miller indices.

Magnetic measurements performed for the Fe_3O_4/GNPs (Figure 3, SM) show that the magnetization presents a fast approach to saturation in the presence of an external magnetic field (reaching saturation for about 5 kOe). The estimated saturation magnetization, at 300 K, is about 102 emu/g Fe_3O_4, which is in the same order of the saturation magnetization for bulk magnetite (92 emu/g), at room temperature[42–44]. The Fe_3O_4/GNPs shows a magnetization of ca. 45 emu/g. This value is higher than for the magnetic composites prepared by covalent bonding (9 emu/g)[45] and by wet-chemical coprecipitation method (28 emu/g)[46]. The coercive field (H_c) for the Fe_3O_4/GNPs is 90 Oe, at room temperature, which evidences ferrimagnetic behaviour characteristic of magnetite nanoparticles in this size range[47].

The FTIR spectrum of the of Fe_3O_4/GNPs also corroborates the presence of the magnetic phase in the material, by the presence of a peak at 591 cm^{-1} corresponding to the stretching vibration of Fe-O in the lattice[46,48]. Apart from the absence of the magnetite peak in the FTIR spectrum of GNPs, the spectra of the carbon precursor and Fe_3O_4/GNPs are similar, with small shifts in the main vibrational bands (Table 2, SM), and some additional peaks in the 1300-1000 cm^{-1} region. The stronger bands are due to the carbon skeleton vibrational modes (C=C and C–H groups) and to oxygen functional groups (hydroxyl groups (–OH) and carbonyl groups (C=O)).

3.2. Removal of Technology-Critical Elements from water

3.2.1.Removal of TCE by Fe_3O_4/GNPs composite and its precursors

The Fe_3O_4/GNPs composite was investigated as sorbent for the removal of TCE from water, and its performance was compared with the performance observed for the isolated

components (Fe_3O_4 and GNPs), after a 24 h period of exposition of equal amounts of GNPs, Fe_3O_4 NPs and Fe_3O_4/GNPs to a ternary solution of La(III), Eu(III) and Tb(III) with an element concentration of 100 μg/L. The results show distinct affinity between materials and the selected TCE, with the Fe_3O_4/GNPs composite showing better capability to remove the selected TCE from water than any of its single components (La: 4.7% (GNPs), 3.1% (Fe_3O_4 NPs) and 15% (Fe_3O_4/GNPs); Eu: 1.2% (GNPs), 0.2% (Fe_3O_4 NPs) and 37.6% (Fe_3O_4/GNPs); Tb: 0.2% (GNPs), 0.1% (Fe_3O_4 NPs) and 35.0% (Fe_3O_4/GNPs)). This can be explained by an increase of active sorption sites in the composite due to the introduction of oxygen moieties in the carbon lattice, because it is well known that trivalent lanthanides are hard Lewis acids with strong chemical affinity for oxygen donors.

3.2.2.Effect of pH on the removal capability of Fe_3O_4/GNPs

The solution pH is one of the most important variables affecting the sorption process at solution-sorbent interfaces, since affects both elements' speciation and the surface charge of the material[49]. Figure 2 displays the removal efficiency of Fe_3O_4/GNPs toward the selected TCE as function of solution pH. After 24h of exposition to a ternary solution of La(III), Eu(III) and Tb(III), equal amounts of Fe_3O_4/GNPs removed from 0 to 94.3±1.1% of La(III), 3.9±0.8 to 94.3±0.9% of Eu(III) and 0 to 94.4±1.0% of Tb(III), by increasing the solution pH from 2 to 10.

These results allow us to conclude that the removal of La(III), Eu(III) and Tb(III) from water by the Fe_3O_4/GNPs depends strongly on pH. A pronounced increase on the removal efficiency occurs for a pH about 6. This behaviour can be explained based on the sorbent surface chemistry (protonation reduction with increasing pH) and aqueous phase chemistry. The isoelectric point (IEP) of the Fe_3O_4/GNPs was found to be 5.2, hence a positive charge exists on the surface of the composite for pH values lower than the IEP, which gradually decreases and attains a negative value for pH values higher than 5.2. When the surface of Fe_3O_4/GNPs is positively charged, the

predominant lanthanide species are the hydrated trivalent ions[50] (La^{3+}, Eu^{3+} and Tb^{3+}). In these acidic conditions, the sorption of the lanthanide cations is not favourable due to electrostatic repulsion and consequently the removal of TCE by the composite is very low (<5%). At pH above 5.2, the number of negatively charged sites at Fe_3O_4/GNPs surface increases, favouring the sorption of cationic species due to electrostatic attraction. As a result, La^{3+}/$La(OH)^{2+}$, Eu^{3+}/$Eu(OH)^{2+}$, EuO^{+} and Tb^{3+}/$Tb(OH)^{2+}$/TbO^{+}/TbO_2H(aq), which are the predominant species[50] for the pH range 5-9, are sorbed onto the Fe_3O_4/GNPs. For instance, at pH 5.8, a value slightly above the IEP, the removal of La(III), Eu(III) and Tb(III) increased from less than 5% to 7, 21 and 17%, respectively, while at pH 9 a significantly high electrostatic attraction exists between the negatively charged surface of the composite and the cationic species, resulting in removal percentages of 61% for La(III) and 79% for Eu(III) and Tb(III). These results highlight that the predominant mechanism involved in the removal of La(III), Eu(III) and Tb(III) by this nanomaterial are electrostatic interactions, with the possible formation of outer-sphere complexes. Wall[51] and Rim[52] have reported that lanthanoids usually form complexes dominated by electrostatic rather than covalent interactions, which are often very stable, as in the case of the oxides. More, the absence of changes in the FTIR and Raman spectra (Figure 4 and 5, SM) after sorption, also support the formation of outer-sphere complexes. The highest removal efficiency (ca. 95%) was observed at pH 10. At this pH, a dark powder remained in the solution after magnetic separation, thus requiring an additional solid-liquid separation process. This suggests that in alkaline conditions probably detachment of the iron oxide NPs occurs in some extent. In fact, at high pH (pH>10) both GNPs and Fe_3O_4 NPs have negative charged surfaces which limits the formation of assemblies via electrostatic interactions. Although for the initial concentration used (100 µg/L) we did not observe (from control essays) co-precipitation of the lanthanide hydroxides, this cannot be ruled out at high pH and for higher initial concentrations the two processes (sorption and

precipitation) might coexist. Although the removal of La(III), Eu(III) and Tb(III) by the Fe_3O_4/GNPs exhibits the same pattern *versus* pH, it is evident an almost coincident profile between Eu(III) and Tb(III). In addition, results point to a lower affinity of the Fe_3O_4/GNPs composite toward La(III) than for Eu(III) or Tb(III). Indeed, for pH values superior to 6, the values found for the selectivity (S_{12},) (calculated by the ratio of the distribution coefficients (q_A/C_A), expressed in molar units[34], where 1 and 2 are different elements), by comparing La(III) and Eu(III), and La(III) and Tb(III), were always lower than 1 and equal to 1 when comparing Eu(III) and Tb(III). Along the lanthanides series the ionic radii get smaller (lanthanide-contraction), and this can explain the dissimilarities between La(III) and, Eu(III) and Tb(III), assuming the same type of metal coordination.

3.2.3.Removal of TCE from unary and ternary solutions by Fe_3O_4/GNPs

Envisaging potential applications of the Fe_3O_4/GNPs to remove TCE from real streams, the capability of this nanomaterial to remove La(III), Eu(III) and Tb(III) from water was evaluated at pH 7.5 ± 0.2, by exposing two doses of composite to unary and ternary solutions for 24h. Unary solutions are important to infer about the sorbent capability toward a given sorbate, but real systems such as rivers or wastewaters, in general contain multiple elements in solution. Accordingly, multi-component adsorption data are essential for the design of treatment and/or recovery processes and, the scarcity of such data in literature led us to carry out studies in ternary solutions. The coexistence of several TCE in solution may result in synergistic, antagonistic or no observable effects on the removal process that should be identified and understood. Figure 3 shows the variation of the normalized concentration(C_A/C_{A0}), over time for each TCE, in the presence of different amounts of Fe_3O_4/GNPs. The symbols represent the C_A/C_{A0} of each TCE for the different sorbent-sorbate(s) systems, while the black dashed line represents the data from the control assays. For clarity, the data are only represented for the first 4h.

In both unary and ternary solutions, and in the presence of the composite, the normalized concentration in solution of each TCE showed a fast decrease in the first minutes, pointing to a high removal rate of TCE from solutions. Then, for a short period of time, evolves into a slower kinetics reaching equilibrium in less than 2h. This behaviour is explained by the large mass transport driving forces observed at the beginning of the experiment, since the composite is free of TCE ions. The decrease on TCE concentration can only be related to the magnetic composite since in its absence, the TCE concentration in solution remained nearly constant. At 4h in unary solutions, the mean values of $C_{\mathrm{A}}/C_{\mathrm{A0}}$ were 0.60±0.02 (La), 0.58±0.05 (Eu) and 0.65±0.05 (Tb) for an amount of 10 mg/L of composite. These values dropped to 0.41±0.05 (La), 0.23±0.04 (Eu) and 0.16±0.07 (Tb) by increasing the dose of composite to 50 mg/L. In ternary solutions, the mean values of $C_{\mathrm{A}}/C_{\mathrm{A0}}$ increased in comparison to the values in unary solutions ranging from ca. 0.40 (Eu and Tb, 50 mg/L of Fe_3O_4/GNPs) to 0.86±0.03 (La, 10 mg/L of Fe_3O_4/GNPs). Overall, it is possible to conclude that regardless the matrix, the equilibrium is reached very fast, the amount of material plays an important role on the efficiency of the removal process and influences the equilibrium time. Moving from unary to ternary solutions there is a reduction on the removal efficiency for all elements, which may be an evidence of competition between TCE for the sorption sites of the nanocomposite. According to Pearson Law[53], the ionic competition is higher between elements from the same class than between elements from different classes. Consequently, the inhibition of the TCE removal process in the ternary solutions could be attributed to this phenomenon. For instance, Zhao et al.[54] also observed a significant reduction on the sorption capacity of a biopolymer toward La(III), Ce(III) and Eu(III) when it was applied to multi-element solutions of those three elements.

3.2.4.Mass balance calculations and kinetic modelling in unary and ternary solutions

The solid loadings, q_A, of each TCE on the Fe_3O_4/GNPs varied with the dose of composite used and with the presence of multiple TCE (Table 1). After 4h exposition, of Fe_3O_4/GNPs to unary solutions, the mean values of q_A were similar between the selected elements for the same experimental conditions and decrease with increasing the concentration of composite. In ternary solutions, the effect of the competition between elements is visible, with the reduction of the solid loadings of each TCE on the Fe_3O_4/GNPs. The extension of the competition effects is not equal to the three TCE, and the removal of La(III) is the most affected, as corroborated by the equilibrium selectivities. The S_{12} values attained between La(III) and Eu(III) (0.41 and 0.30, respectively for 10 and 50 mg/g Fe_3O_4/GNPs) and between La(III) and Tb(III) (0.47 and 0.32, respectively for 10 and 50 mg/g Fe_3O_4/GNPs) have shown that the composite has higher affinity toward Eu(III) and Tb(III) than for La(III). For Eu(III) and Tb(III), the selectivity values were around 1.0, for both doses of composite. Overall, with respect to the TCE here considered (in ternary systems), as for the S_{12} values calculated, the equilibrium selectivity of Fe_3O_4/GNPs composite follows the order Tb≈ Eu>La. The higher equilibrium selectivity of Tb and Eu may be related to the lanthanide-contraction, i.e. the decrease of ionic radii with the increase of atomic number. The Tb^{3+} and Eu^{3+} ions, of smaller ionic size, may reach binding sites inaccessible to the larger La^{3+} ions.

The solid loadings of each TCE on the Fe_3O_4/GNPs (q_A, mg/g) *versus* time, for unary and ternary solutions, is represented in Figure 4. For all sorbent-sorbate(s) systems the kinetic profiles are characterized by an abrupt increase of the solid loading of each TCE in the composite, followed by a less pronounced increase, reaching a horizontal branch (*plateau*). Kinetic models were used to fit the experimental data. Only the curves that best fit the removal of La(III), Eu(III) and Tb(III) are presented in Figure 4, and the best-fit parameters for each data set are summarized in Table 2. Overall, the fitting curves based on three kinetic models, namely, pseudo-first order, pseudo-second order and Elovich provided good adjustments to the experimental data, for all the studied

sorbent-sorbate(s) systems, with most of the absolute average relative deviation below 5% and the coefficient of determination (R^2) above 0.90. Considering that the fitting of the pseudo-second order model presents the highest coefficient of determination for the largest number of systems, this discussion will be based on the kinetic parameters of this model.

The kinetic profile of each TCE reveals that the equilibrium is reached very quickly when exposing 50 mg/L of Fe_3O_4/GNPs to both unary and ternary solutions (5 to 15 min), with a longer period of time required (1 to 2h) to attain equilibrium for 10 mg/L of composite. For the TCE considered here, in unary systems, and considering the k_2 shown in Table 2, the sorption rate onto Fe_3O_4/GNPs depends on the amount of sorbent, i.e., the TCE removal process is faster for high doses of Fe_3O_4/GNPs, and follows this order for each dose of composite, La≈Eu≈Tb (10 mg/L) and La>Eu>Tb (50 mg/L). The estimation of the $q_{\mathrm{A,e}}$ values by the pseudo-second order match accurately with the experimental equilibrium values (relative errors lower than 8%).

Concerning the variation of the rate constant in the presence of multiple TCE, one can conclude that except for La(III), there are no substantial differences and the values are of the same order of magnitude. However, in this scenario and for both amounts of sorbent, the sorption rate of TCE onto Fe_3O_4/GNPs follows a clear order: La>Eu≈Tb. For Eu(III) and Tb(III) the estimation of the $q_{\mathrm{A,e}}$ values by the pseudo-second order matches accurately the experimental equilibrium values (relative errors lower than 5%), while for La(III) the values were higher (relative errors of 14 and 10%, respectively, for 10 and 50 mg/L of composite).

Overall, the removal kinetics is mainly affected by the amount of sorbent, and although mechanisms cannot be directly assigned based on kinetic modelling, the pseudo-second order model, which best described these results, has general application to describe chemisorption processes. Computing the kinetic selectivities of the three TCE (values estimated by the ratios between the removal rates), it is interested to notice that although La(III) displays an equilibrium

selectivity lower than Eu(III) and Tb(III), it has the highest kinetic selectivity. The high kinetic selectivity of La(III) may be related to its lower atomic mass. Being the lightest of the three TCE, the La ions diffuse fast in the solution, reaching the sorption sites quicker than Eu and Tb ions.

3.2.5.Sorption equilibrium and modelling in unary and ternary solutions

For a quantitative determination of the sorption capacity of the Fe_3O_4/GNPs, different amounts of composite were exposed to unary and ternary solutions of La(III), Eu(III) and Tb(III) for 24h, and mathematical functions of the equilibrium data between the concentration of the TCE ions in the liquid and solid phases were evaluated. Figure 5 displays the equilibrium data for the different sorbent-sorbate(s) systems at 22±1 °C. All isotherms exhibit a very unfavourable trend, with an almost square convex shape to the concentration axis ($C_{\mathrm{A,e}}$). In terms of the theoretical classification of BDDT (Brunauer, Deming, Deming, Teller), their shape falls within type III, and according to the Giles classification[55], the isotherms follow S-type curve pattern. This very unfavourable trend was also found recently in the sorption of Hg(II) onto cork stoppers powder[37]. The most noteworthy feature of these systems is that sorption becomes easier as concentration rises. As more solute is sorbed, the easier it is for additional amounts to become fixed, which implies a side-by side association between sorbed species, helping to hold them to the surface (the so called “co-operative adsorption’’)[55]. According to Giles[55], the S curve usually appears when the solute molecule is monofunctional, has moderate intermolecular attraction, causing it to pack vertically in regular array in the sorbed layer, and meets strong competition, for substrate sites, from molecules of the solvent or of another sorbed species.

Comparing the isotherms obtained for the unary and ternary systems occur a shift to high values on the concentration value ($C_{\mathrm{A,e}}$) when the sorption starts to rise increases, reflecting the ionic competition in the ternary system. These $C_{\mathrm{A,e}}$ values follow the order Tb(III)≈Eu(III)<La(III).

Moreover, in the range of experimental conditions used, the highest $q_{A,e}$ values recorded for the unary solutions were 16.2 (La), 17.9 (Eu) and 23.0 mg/g (Tb), and 3.8 (La), 11.9 (Eu) and 12.5 mg/g (Tb) for the ternary solution. Even though these values do not represent the maximum sorption capacity of Fe_3O_4/GNPs, they are similar or higher than some values report in literature as the maximum sorption capacity of sorbents toward some lanthanoids. For instance, Zhao et al.[54] reported that maximum sorption capacity of a biopolymer in mono-elementary solution of La(III), Ce(III) and Eu(III) with initial element concentrations of 4 to 200 mg/L, was 47 (La), 49 (Ce) and 55 mg/g (Eu), while in multi-elementary solutions was 5 (La), 10 (Ce) and 30 mg/g (Eu). Carvalho et al.[56] reported a maximum sorption capacity of magnetite nanoparticles with APTMS for Eu(III) of 33 mg/g, using a solution with initial element concentration of 15.2 mg/L. Other authors[57–60], reported maximum sorption capacities for Eu (0.003 to 1.52 mg/g) and Tb (0.049 to 0.11 mg/g) much lower than the ones found within this study. The trend observed for the different sorbent-sorbate(s) systems is difficult to be fitted by the simplest equilibrium models that are widely described in the literature. The mathematical function that was able to describe, in some extension, the equilibrium data of some of these systems is given by the Freundlich model (R^2 ranged from 0.66 to 0.90). The magnitude of the fitting parameters (Table 3) confirms the unfavourable nature of the equilibrium sorption (n values <1).

3.3. Recovery of Technology-Critical Elements from Fe_3O_4/GNPs

The recovery of TCE was investigated by means of Fe_3O_4/GNPs regeneration, by its treatment with 0.1 mol/L HNO_3 for a 24h of exposition to a ternary solution of La(III), Eu(III) and Tb(III). The TCE removal efficiency of the composite after each regeneration cycle was also evaluated. As shown in Figure 6, during the subsequent cycles, the recovery efficiency of the TCE ranged from 82 to 92% for La(III), 88 to 104% for Eu(III) and 82 to 97% for Tb(III), suggesting that 0.1 mol/L HNO_3 is

an effective eluent for the recovery of these elements from the composite. More, the capability of the composite to remove the selected TCE from water was rarely affected since the values of the removal efficiency remained nearly constant during all cycles, confirming also the stability of the composite in diluted HNO_3, which was also corroborate by Raman spectroscopy (Figure 5, SM). The results allow us to state that Fe_3O_4/GNPs is a recyclable sorbent and can be used in several sorption/desorption cycles.

4. Conclusions

Hybrid nanocomposites were successfully prepared by electrostatic assembly of graphite nanoplatelets and colloidal magnetite nanoparticles. These composites exhibited good sorption properties towards trivalent lanthanides (La, Eu and Tb), using diluted unary and ternary model aqueous solutions, under the experimental conditions described here. It is suggested that the sorption mechanism is mainly controlled by electrostatic interactions, which turns this process useful for pH values higher than 5.2, which is the experimental isoelectric point of the composite. The maximum solid loading achieved was 230 μg/mg, at pH 7.5 and using 2 mg/L of composite. In ternary solutions of TCE, the Fe_3O_4/GNPs removed preferentially Eu(III) and Tb(III) species as compared to La(III), but this type of sorption affinity was not so obvious in unary systems. Moreover, for consecutive removal-reuse cycles applied to ternary solutions of TCE (100 μg/L) and for the experimental conditions employed (pH 7.5, 250mg/L of Fe_3O_4/GNPs and using 0.1M HNO_3 as eluent solution), it was observed good potential for recyclability without loss of efficiency. This sequential process might constitute a way to recover TCE from diluted and neutral aqueous streams, which has been a main limitation encountered in the recovery and reuse of these critical elements.

Conflicts of interest

There are no conflicts to declare.

Acknowledgements

This work was developed within the scope of the project CICECO-Aveiro Institute of Materials, FCT Ref. UID/CTM/50011/2019, financed by national funds through the FCT/MCTES. C.B. Lopes and S. Fateixa thanks the national funds (OE), through FCT, I.P., in the scope of the framework contract foreseen in the UID/CTM/50011/2019numbers 4, 5 and 6 of the article 23, of the Decree-Law 57/2016, of August 29, changed by Law 57/2017, of July 19.

References

[1] A. Cobelo-García, M. Filella, P. Croot, C. Frazzoli, G. Du Laing, N. Ospina-Alvarez, S. Rauch, P. Salaun, J. Schäfer, S. Zimmermann, COST action TD1407: network on technology-critical elements (NOTICE)—from environmental processes to human health threats, Environ. Sci. Pollut. Res. 22 (2015) 15188–15194. doi:10.1007/s11356-015-5221-0.

[2] C.E.D. Cardoso, J.C. Almeida, C.B. Lopes, T. Trindade, C. Vale, E. Pereira, Recovery of Rare Earth Elements by Carbon-Based Nanomaterials — A Review, Nanomaterials. 9 (2019) 814. doi:10.3390/nano9060814.

[3] M. Filella, Fate of technology-critical elements in the environment, with a focus on less-studied ones, in: 18 Th Int. Conf. Heavy Met. Environ., Ghent, 2016: pp. 1–2.

[4] The Geological Society of London, Rare earth elements-A briefing note by the Geological Society of London, London, 2011.

[5] M.I. Leybourne, K.H. Johannesson, Rare earth elements (REE) and yttrium in stream waters, stream sediments, and Fe-Mn oxyhydroxides: Fractionation, speciation, and controls over REE + Y patterns in the surface environment, Geochim. Cosmochim. Acta. 72 (2008) 5962–5983. doi:10.1016/j.gca.2008.09.022.

[6] S. Kulaksiz, M. Bau, Anthropogenic dissolved and colloid/nanoparticle-bound samarium, lanthanum and gadolinium in the Rhine River and the impending destruction of the natural rare earth element distribution in rivers, Earth Planet. Sci. Lett. 362 (2013) 43–50. doi:10.1016/j.epsl.2012.11.033.

[7] G. Klaver, M. Verheul, I. Bakker, E. Petelet-Giraud, P. Négrel, Anthropogenic Rare Earth Element in rivers: GADOLINIUM and lanthanum. Partitioning between the dissolved and particulate phases in the Rhine River and spatial propagation through the Rhine-Meuse Delta (the Netherlands), Appl. Geochemistry. 47 (2014) 186–197.

doi:10.1016/j.apgeochem.2014.05.020.

[8] V. Funari, S.N.H. Bokhari, L. Vigliotti, T. Meisel, R. Braga, The rare earth elements in municipal solid waste incinerators ash and promising tools for their prospecting, J. Hazard. Mater. 301 (2016) 471–479. doi:10.1016/j.jhazmat.2015.09.015.

[9] V. Funari, R. Braga, S.N.H. Bokhari, E. Dinelli, T. Meisel, Solid residues from Italian municipal solid waste incinerators: A source for "'critical'" raw materials, Waste Manag. 45 (2015) 206–216. doi:10.1016/j.wasman.2014.11.005.

[10] L.S. Morf, R. Gloor, O. Haag, M. Haupt, S. Skutan, F. Di Lorenzo, D. Böni, Precious metals and rare earth elements in municipal solid waste - Sources and fate in a Swiss incineration plant, Waste Manag. 33 (2013) 634–644. doi:10.1016/j.wasman.2012.09.010.

[11] A. Tsamis, M. Coyne, Recovery of Rare Earths from Electronic wastes: An opportunity for High-Tech SMEs, 2015. http://www.europarl.europa.eu/RegData/etudes/STUD/2015/518777/IPOL_STU(2015)518777_EN.pdf.

[12] S. Stankovich, D.A. Dikin, R.D. Piner, K.A. Kohlhaas, A. Kleinhammes, Y. Jia, Y. Wu, S.B.T. Nguyen, R.S. Ruoff, Synthesis of graphene-based nanosheets via chemical reduction of exfoliated graphite oxide, Carbon N. Y. 45 (2007) 1558–1565. doi:10.1016/j.carbon.2007.02.034.

[13] K. Kalaitzidou, H. Fukushima, L.T. Drzal, Multifunctional polypropylene composites produced by incorporation of exfoliated graphite nanoplatelets, Carbon N. Y. 45 (2007) 1446–1452. doi:10.1016/j.carbon.2007.03.029.

[14] S. Nasimul Alam, N. Sharma, B. Chandra Ray, S. Yadav, K. Biswas, Effect of graphite nanoplatelets on the mechanical properties of alumina-based composites, Ceram. Int. 43 (2017) 11376–11389. doi:10.1016/j.ceramint.2017.05.345.

[15] G. Li, X. Tian, X. Xu, C. Zhou, J. Wu, Q. Li, L. Zhang, F. Yang, Y. Li, Fabrication of robust and highly thermally conductive nanofibrillated cellulose/graphite nanoplatelets composite papers, Compos. Sci. Technol. 138 (2017) 179–185. doi:10.1016/j.compscitech.2016.12.001.

[16] N. Zanato, L. Talamini, T.R. Silva, I.C. Vieira, Microcystin-LR label-free immunosensor based on exfoliated graphite nanoplatelets and silver nanoparticles, Talanta. 175 (2017) 38–45. doi:10.1016/j.talanta.2017.07.021.

[17] A.K. Mishra, L. Huang, TiO2-decorated graphite nanoplatelet nanocomposites for high-temperature sensor applications, Small. 11 (2015) 361–366. doi:10.1002/smll.201401418.

[18] T. Zhou, D. Chen, J. Jiu, T.T. Nge, T. Sugahara, S. Nagao, H. Koga, M. Nogi, K. Suganuma, X. Wang, X. Liu, P. Cheng, T. Wang, D. Xiong, Electrically conductive bacterial cellulose composite membranes produced by the incorporation of graphite nanoplatelets in pristine bacterial cellulose membranes, Express Polym. Lett. 7 (2013) 756–766. doi:10.3144/expresspolymlett.2013.73.

[19] C.A. Crock, A.R. Rogensues, W. Shan, V. V. Tarabara, Polymer nanocomposites with graphene-based hierarchical fillers as materials for multifunctional water treatment membranes, Water Res. 47 (2013) 3984–3996. doi:10.1016/j.watres.2012.10.057.

[20] M.N. Carvallho, K.S. Da Silva, D.C.S. Sales, E.M.P.L. Freire, M.A.M. Sobrinho, M.G. Ghislandi, Dye removal from textile industrial effluents by adsorption on exfoliated graphite nanoplatelets: Kinetic and equilibrium studies, Water Sci. Technol. 73 (2016) 2189–2198. doi:10.2166/wst.2016.073.

[21] A.K. Mishra, S. Ramaprabhu, Magnetite decorated graphite nanoplatelets as cost effective CO2 adsorbent, J. Mater. Chem. 21 (2011) 7467–7471. doi:10.1039/c1jm10996k.

[22] R. Mukkabla, P. Meduri, M. Deepa, P. Ghosal, Durable Li-S batteries with nano-

sulfur/graphite nanoplatelets composites, Chem. Eng. J. 303 (2016) 369–383. doi:10.1016/j.cej.2016.05.146.

[23] W. Meng, K.H. Khayat, Mechanical properties of ultra-high-performance concrete enhanced with graphite nanoplatelets and carbon nanofibers, Compos. Part B Eng. 107 (2016) 113–122. doi:10.1016/j.compositesb.2016.09.069.

[24] L. Gardella, S. Colonna, A. Fina, O. Monticelli, A Novel Electrostimulated Drug Delivery System Based on PLLA Composites Exploiting the Multiple Functions of Graphite Nanoplatelets, ACS Appl. Mater. Interfaces. 8 (2016) 24909–24917. doi:10.1021/acsami.6b08808.

[25] C.B. Lopes, P. Figueira, D.S. Tavares, Z. Lin, A.L. Daniel-da-Silva, A.C. Duarte, J. Rocha, T. Trindade, E. Pereira, Core-shell magnetite-silica dithiocarbamate-derivatised particles achieve the Water Framework Directive quality criteria for mercury in surface waters, Environ. Sci. Pollut. Res. 20 (2013). doi:10.1007/s11356-013-1615-z.

[26] P.C. Pinheiro, D.S. Tavares, A.L. Daniel-Da-Silva, C.B. Lopes, E. Pereira, J.P. Araújo, C.T. Sousa, T. Trindade, Ferromagnetic sorbents based on nickel nanowires for efficient uptake of mercury from water, ACS Appl. Mater. Interfaces. 6 (2014). doi:10.1021/am5010865.

[27] P.I. Girginova, A.L. Daniel-da-Silva, C.B. Lopes, P. Figueira, M. Otero, V.S. Amaral, E. Pereira, T. Trindade, Silica coated magnetite particles for magnetic removal of Hg2+ from water, J. Colloid Interface Sci. 345 (2010) 234–240. doi:10.1016/j.jcis.2010.01.087.

[28] D.S. Tavares, A.L. Daniel-Da-Silva, C.B. Lopes, N.J.O. Silva, V.S. Amaral, J. Rocha, E. Pereira, T. Trindade, Efficient sorbents based on magnetite coated with siliceous hybrid shells for removal of mercury ions, J. Mater. Chem. A. 1 (2013). doi:10.1039/c3ta10914c.

[29] P. Figueira, C.B. Lopes, A.L. Daniel-da-Silva, E. Pereira, A.C. Duarte, T. Trindade, Removal of mercury (II) by dithiocarbamate surface functionalized magnetite particles: Application to

synthetic and natural spiked waters, Water Res. 45 (2011). doi:10.1016/j.watres.2011.08.057.

[30] T. Fernandes, S. Soares, T. Trindade, A. Daniel-da-Silva, Magnetic Hybrid Nanosorbents for the Uptake of Paraquat from Water, Nanomaterials. 7 (2017) 68. doi:10.3390/nano7030068.

[31] S.F. Soares, T.R. Simões, T. Trindade, A.L. Daniel-da-Silva, Highly Efficient Removal of Dye from Water Using Magnetic Carrageenan/Silica Hybrid Nano-adsorbents, Water. Air. Soil Pollut. 228 (2017). doi:10.1007/s11270-017-3281-0.

[32] U. Schwertmann, R.M. Cornell, Magnetite, in: Iron Oxides Lab. Prep. Charact., Wiley-VCH Verlag GmbH, Weinheim, 2000: pp. 135–140. doi:10.1002/9783527613229.ch11.

[33] Q. Han, Z. Wang, J. Xia, S. Chen, X. Zhang, M. Ding, Facile and tunable fabrication of Fe3O4/graphene oxide nanocomposites and their application in the magnetic solid-phase extraction of polycyclic aromatic hydrocarbons from environmental water samples, Talanta. 101 (2012) 388–395. doi:10.1016/j.talanta.2012.09.046.

[34] S.P. Cardoso, C.B. Lopes, E. Pereira, A.C. Duarte, C.M. Silva, Competitive removal of $Cd^{2+}$and Hg^{2+}ions from water using titanosilicate ETS-4: Kinetic behaviour and selectivity, Water. Air. Soil Pollut. 224 (2013). doi:10.1007/s11270-013-1535-z.

[35] D.S. Tavares, C.B. Lopes, J.P. Coelho, M.E. Sánchez, A.I. Garcia, A.C. Duarte, M. Otero, E. Pereira, Removal of arsenic from aqueous solutions by sorption onto sewage sludge-based sorbent, Water. Air. Soil Pollut. 223 (2012). doi:10.1007/s11270-011-1025-0.

[36] P. Figueira, M.A.O. Lourenço, E. Pereira, J.R.B. Gomes, P. Ferreira, C.B. Lopes, Periodic mesoporous organosilica with low thiol density - A safer material to trap Hg(II) from water, J. Environ. Chem. Eng. 5 (2017). doi:10.1016/j.jece.2017.09.032.

[37] C.B. Lopes, J.R. Oliveira, L.S. Rocha, D.S. Tavares, C.M. Silva, S.P. Silva, N. Hartog, A.C.

Duarte, E. Pereira, Cork stoppers as an effective sorbent for water treatment: The removal of mercury at environmentally relevant concentrations and conditions, Environ. Sci. Pollut. Res. 21 (2014) 2108–2121. doi:10.1007/s11356-013-2104-0.

[38] S. Lagergren, About the theory of so-called adsorption of soluble substances, K. Sven. Vetenskapsakademiens Handl. 24 (1898) 1–39.

[39] Y.S. Ho, G. McKay, Pseudo-second order model for sorption processes, Process Biochem. 34 (1999) 451–465. doi:10.1016/S0032-9592(98)00112-5.

[40] C. Aharoni, F.C. Tompkins, Kinetics of Adsorption and Desorption and the Elovich Equation, in: 1970: pp. 1–49. doi:10.1016/S0360-0564(08)60563-5.

[41] H.M.F. Freundlich, Zeitschrift fuer Physikalische Chemie, Stoechiometrie und Verwandtschaftslehre, J. Phys. Electrochem. 57 (1906) 385–470.

[42] R.M. Cornell, U. Schwertmann, The Iron Oxides: Structure, Properties, Reactions, Occurences and Uses, Wiley-VCH Verlag GmbH & Co. KGaA, 2003. doi:10.1002/3527602097.

[43] M. Matsui, S. Tōdō, S. Chikazumi, Magnetization of low temperature phase of Fe3O4, J. Phys. Soc. Japan. 43 (1977) 47–52.

[44] A.R. Muxworthy, E. McClelland, Review of the low-temperature magnetic properties of magnetite from a rock magnetic perspective, Geophys. J. Int. 140 (2000) 101–114. doi:10.1046/j.1365-246X.2000.00999.x.

[45] F. He, J. Fan, D. Ma, L. Zhang, C. Leung, H.L. Chan, The attachment of Fe3O4 nanoparticles to graphene oxide by covalent bonding, Carbon N. Y. 48 (2010) 3139–3144. doi:10.1016/j.carbon.2010.04.052.

[46] W. Jiao, M. Shioya, R. Wang, F. Yang, L. Hao, Y. Niu, W. Liu, L. Zheng, F. Yuan, L. Wan, X. He, Improving the gas barrier properties of Fe3O4/graphite nanoplatelet reinforced

nanocomposites by a low magnetic field induced alignment, Compos. Sci. Technol. 99 (2014) 124–130. doi:10.1016/j.compscitech.2014.05.022.

[47] X. Batlle, A. Labarta, Finite-size effects in fine particles: Magnetic and transport properties, J. Phys. D. Appl. Phys. 35 (2002) 15–42.

[48] L. Wei, F. Wu, D. Shi, C. Hu, X. Li, W. Yuan, J. Wang, J. Zhao, H. Geng, H. Wei, Y. Wang, N. Hu, Y. Zhang, Spontaneous intercalation of long-chain alkyl ammonium into edge-selectively oxidized graphite to efficiently produce high-quality graphene, Sci. Rep. 3 (2013) 2636. doi:10.1038/srep02636.

[49] C.B. Lopes, M. Otero, Z. Lin, C.M. Silva, E. Pereira, J. Rocha, A.C. Duarte, Effect of pH and temperature on Hg2+ water decontamination using ETS-4 titanosilicate, J. Hazard. Mater. 175 (2010). doi:10.1016/j.jhazmat.2009.10.025.

[50] N. Takeno, Atlas of Eh-pH diagrams Intercomparison of thermodynamic databases, Natl. Inst. Adv. Ind. Sci. Technol. Tokyo. (2005) 285.

[51] F. Wall, Rare earth elements, in: G. Gunn (Ed.), Crit. Met. Handb., First Edit, John Wiley & Sons, Ltd., Penryn, UK, 2014: pp. 312–339.

[52] K.T. Rim, Trends in Occupational Toxicology of Rare Earth Elements, in: G. Pagano (Ed.), Rare Earth Elem. Hum. Environ. Heal. Crossroads between Toxic. Saf., Pan Stanford publishing Pte. Ltd, Singapore, 2017: p. 256.

[53] R.G. Pearson, Hard and Soft Acids and Bases, J. Am. Chem. Soc. 85 (1963) 3533–3539. doi:10.1021/ja00905a001.

[54] F. Zhao, E. Repo, Y. Meng, X. Wang, D. Yin, M. Sillanpää, An EDTA-β-cyclodextrin material for the adsorption of rare earth elements and its application in preconcentration of rare earth elements in seawater, J. Colloid Interface Sci. 465 (2016) 215–224. doi:10.1016/j.jcis.2015.11.069.

[55] C.H. Giles, T.H. MacEwan, S.N. Nakhwa, D. Smith, 786. Studies in adsorption. Part XI. A system of classification of solution adsorption isotherms, and its use in diagnosis of adsorption mechanisms and in measurement of specific surface areas of solids, J. Chem. Soc. (1960) 3973–3993. doi:10.1039/JR9600003973.

[56] R.S. Carvalho, A.L. Daniel-Da-Silva, T. Trindade, Uptake of Europium(III) from Water using Magnetite Nanoparticles, Part. Part. Syst. Charact. 33 (2016) 150–157. doi:10.1002/ppsc.201500170.

[57] D.D. Shao, Q.H. Fan, J.X. Li, Z.W. Niu, W.S. Wu, Y.X. Chen, X.K. Wang, Removal of Eu(III) from aqueous solution using ZSM-5 zeolite, Microporous Mesoporous Mater. 123 (2009) 1–9. doi:10.1016/j.micromeso.2009.03.043.

[58] A.C. Texier, Y. Andrès, C. Faur-Brasquet, P. Le Cloirec, Fixed-bed study for lanthanide (La, Eu, Yb) ions removal from aqueous solutions by immobilized Pseudomonas aeruginosa: Experimental data and modelization, Chemosphere. 47 (2002) 333–342. doi:10.1016/S0045-6535(01)00244-2.

[59] Z. Guo, Y. Li, S. Pan, J. Xu, Fabrication of Fe3O4@cyclodextrin magnetic composite for the high-efficient removal of Eu(III), J. Mol. Liq. 206 (2015) 272–277. doi:10.1016/j.molliq.2015.02.034.

[60] R. Akkaya, Terbium adsorption onto polyhydroxyethylmethacrylate-hydroxyapatite composite and its modified composition by phytic acid, Desalin. Water Treat. 52 (2014) 1440–1447. doi:10.1080/19443994.2013.793922.

Table 1: Solid loadings (mean±standard deviation), of each TCE after 4h of exposition to unary and ternary solutions.

		q_A (mg/g)					
		La(III)		Eu(III)		Tb(III)	
		---	+Eu(III) +Tb(III)	---	+La(III) +Tb(III)	---	+La(III) +Eu(III)
10 mg/L	$q_{A,4h}$	3.84±0.35	1.24±0.42	3.46 ±0.29	2.21 ±0.34	3.28±0.34	2.04±0.42
50 mg/L	$q_{A,4h}$	1.16±0.08	0.65±0.02	1.36 ±0.12	1.19 ±0.08	1.21±0.15	1.16±0.07

Table 2: Optimized kinetic parameters (±standard error) of the pseudo-second order model for the different sorbent-sorbate(s) systems.

		La(III)		Eu(III)		Tb(III)	
		---	+Eu(III) +Tb(III)	---	+La(III) +Tb(III)	---	+La(III) +Eu(III)
10 mg/L	k_2	5.31±0.91	35.0±18.2	7.84±2.78	4.62±1.48	4.22±1.22	3.66±1.28
	$q_{A,e}$	3.54±0.08	1.01±0.05	3.21±0.12	1.90±0.11	3.14±0.13	1.88±0.13
	R^2	0.984	0.920	0.953	0.928	0.961	0.912
	$S_{y.x}$	0.13	0.09	0.23	0.15	0.20	0.17
50 mg/L	k_2	880±2014	146±22	62.7±8.7	53.1±8.0	41.5±5.1	48.2±9.3
	$q_{A,e}$	1.15±0.01	0.584±0.00	1.25±0.01	1.11±0.01	1.16±0.01	1.09±0.01
	R^2	0.994	0.998	0.998	0.996	0.997	0.993
	$S_{y.x}$	0.03	0.01	0.02	0.02	0.02	0.03

k_2 (g/mg h); $q_{A,e}$ (mg/g)

Table 3: Optimized isotherm parameters (±standard error) for the different sorbent-sorbate(s) systems.

		La(III)		Eu(III)		Tb(III)	
		---	+Eu(III) +Tb(III)	---	+La(III) +Tb(III)	---	+La(III) +Eu(III)
Freundlich	k_F	5.75×10^{-8} ±1.32×10^{-7}	n.a.	5.31×10^{-6} ±3.32×10^{-5}	3.32×10^{-27} ±3.32×10^{-28}	4.30×10^{-6} ±2.67×10^{-5}	1.03×10^{-28} ±1.12×10^{-29}
	n	0.22±0.03	n.a.	0.28±0.12	0.07±0.01	0.26±0.11	0.06±0.01
	R^2	0.906	n.a.	0.661	0.847	0.678	0.806
	$S_{y.x}$	1.33	n.a.	3.16	1.43	3.77	1.60

k_F ($mg^{1-1/n}L^{1/n}/g$); n.a. not applicable

Figure 1. TEM images of graphite nanoplatelets (a), Fe_3O_4 (b) and Fe_3O_4/GNPs (c).

Figure 2. Effect of pH on TCE removal from ternary solution. $C_{A,0}$=100 µg/L and m/V=50 mg/L.

Figure 3. Normalized concentration of La, Eu and Tb with time, in unary and ternary solutions, for different doses of Fe_3O_4/GNPs. Results are expressed as mean values and error bars represent the standard deviation of duplicates. $C_{A,0}$=100 µg/L, pH 7.5±0.2 and m/V=10 mg/L (full symbols) or 50 mg/L (open symbols). The black dashed line represents the normalized concentration of each TCE in control.

Figure 4. Experimental solid loading (symbols) and pseudo-second order model fit (lines) of La, Eu and Tb with time, in unary and ternary solutions, for different doses of Fe_3O_4/GNPs. Results are expressed as mean values and error bars represent the standard deviation of duplicates. $C_{A,0}$=100 µg/L, pH 7.5±0.2 and m/V=10 mg/L (full symbols) or 50 mg/L (open symbols).

Figure 5. Experimental equilibrium data (symbols) and Freundlich isotherm (lines) for each TCE-Fe_3O_4/GNPs system at 22±1 °C, in unary (full symbols) and ternary (open symbols) solutions. Results are expressed as mean values and error bars represent the standard deviation of duplicates. $C_{A,0}$=100 µg/L, pH 7.5±0.2, m/V=2 - 60 mg/L.

Figure 6. Sorption/desorption cycles of TCE using Fe_3O_4/GNPs as sorbent and 0.1 M HNO_3 as eluent: (a) removal of TCE from ternary solution, and (b) recovery of TCE from Fe_3O_4/GNPs. Results are expressed as mean values and error bars represent the standard deviation of duplicates. $C_{A,0}$=100 µg/L, pH 7.5±0.2, m/V=250 mg/L.

Fig.1

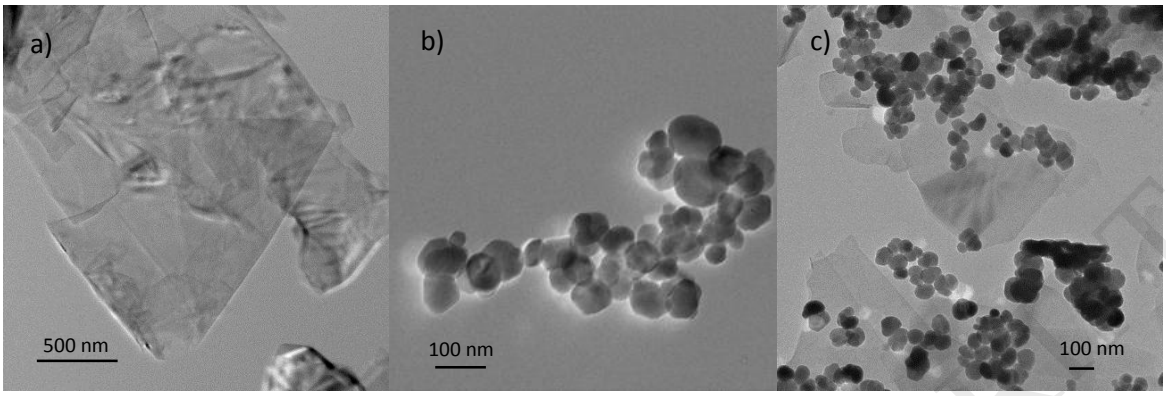

Fig.2

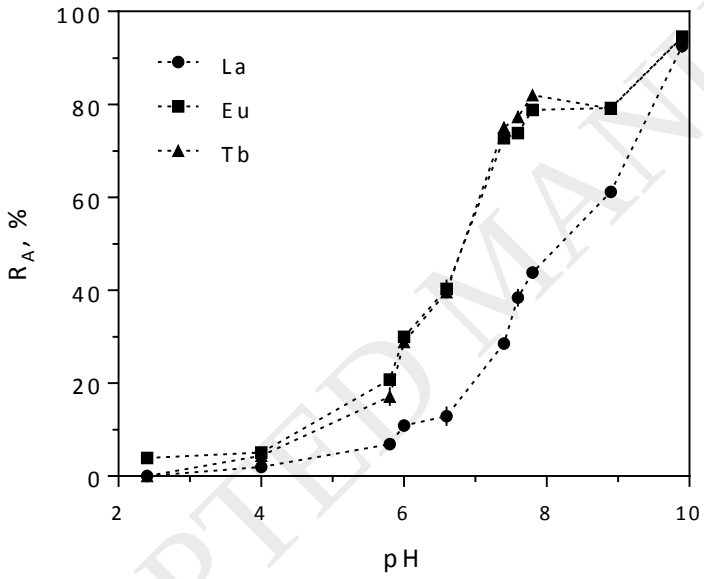

Fig. 3

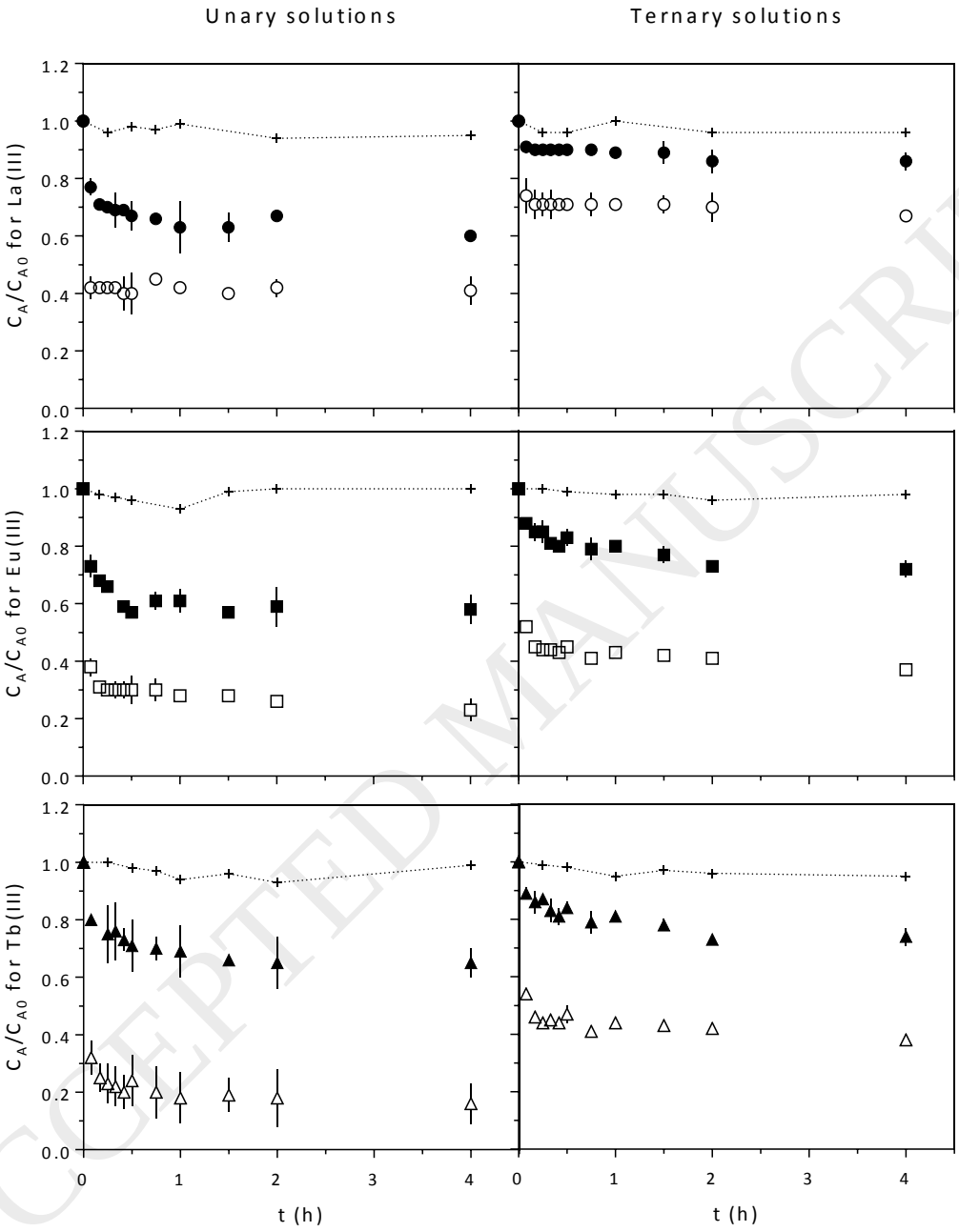

Fig. 4

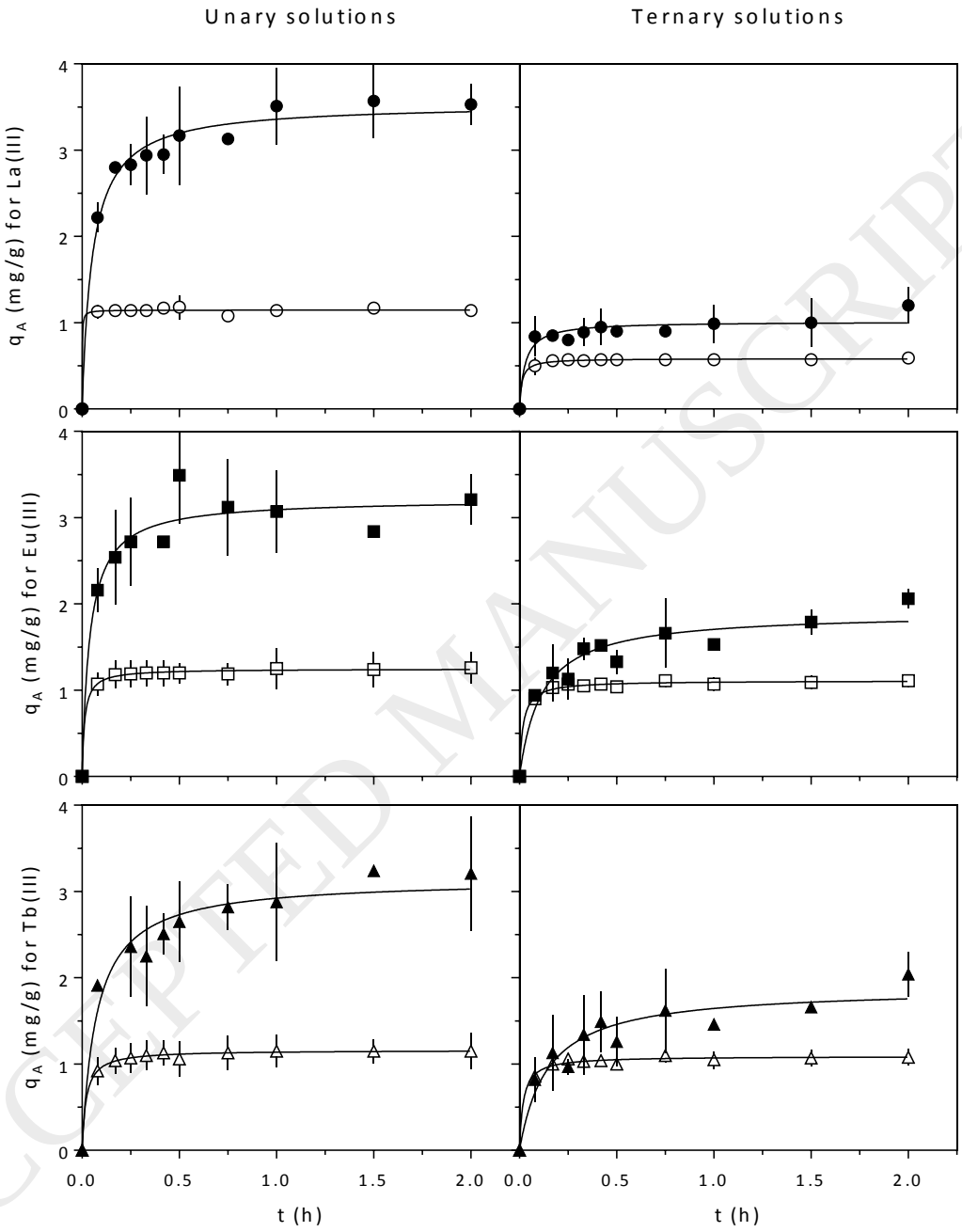

Fig.5

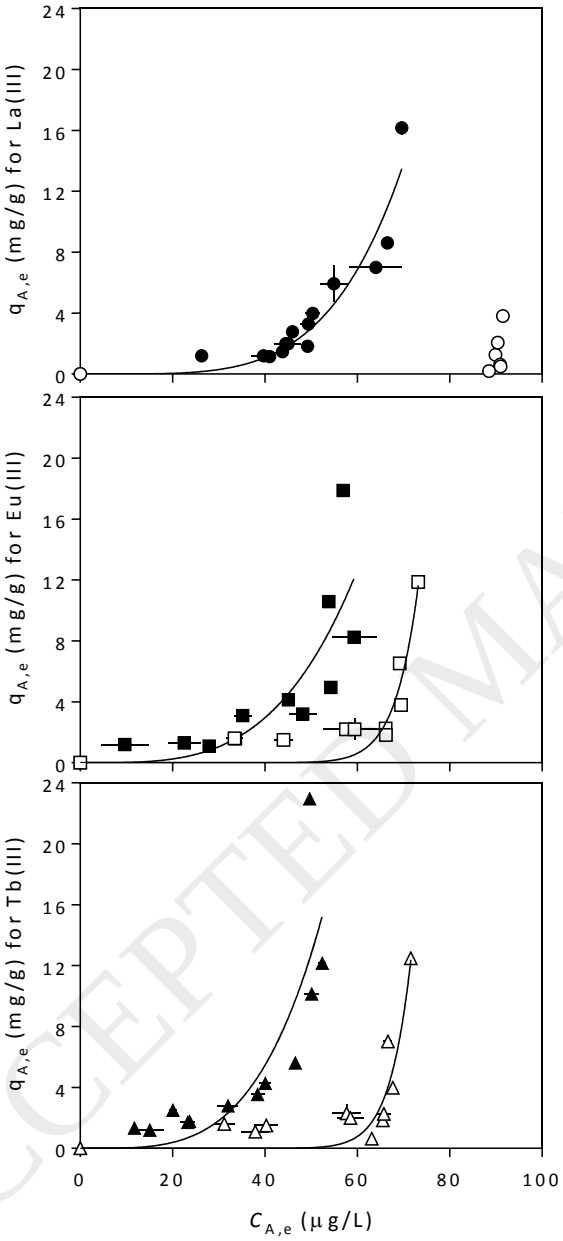

Fig. 6